![USGS logo](science for a changing world)

Three-Dimensional Geologic Map of the Hayward Fault Zone, San Francisco Bay Region, California

By G.A. Phelps, R.W. Graymer, R.C. Jachens, D.A. Ponce, R.W. Simpson, and C.M. Wentworth

Pamphlet to accompany
Scientific Investigations Map 3045

U.S. Department of the Interior
U.S. Geological Survey

Contents

Tables

Figures

Appendixes

THREE-DIMENSIONAL GEOLOGIC MAP OF THE HAYWARD FAULT ZONE, SAN FRANCISCO BAY REGION, CALIFORNIA

By G.A. Phelps, R.W. Graymer, R.C. Jachens, D.A. Ponce, R.W. Simpson, and C.M. Wentworth

Abstract

A three-dimensional (3D) geologic map of the Hayward Fault zone was created by integrating the results from geologic mapping, potential field geophysics, and seismology investigations. The map volume is 100 km long, 20 km wide, and extends to a depth of 12 km below sea level. The map volume is oriented northwest and is approximately bisected by the Hayward Fault. The complex geologic structure of the region makes it difficult to trace many geologic units into the subsurface. Therefore, the map units are generalized from 1:24000-scale geologic maps. Descriptions of geologic units and structures are offered, along with a discussion of the methods used to map them and incorporate them into the 3D geologic map. The map spatial database and associated viewing software are provided. Elements of the map, such as individual fault surfaces, are also provided in a non-proprietary format so that the user can access the map via open-source software. The sheet accompanying this manuscript shows views taken from the 3D geologic map for the user to access. The 3D geologic map is designed as a multi-purpose resource for further geologic investigations and process modeling.

Scope and Purpose of this report

The purpose of this new map is to compile the best available data on: 1) identity and subsurface distribution of bedrock units, 2) sedimentary deposits, and 3) geologic structures at a regional scale, and to integrate the data into a 3D map. The 3D nature of the map allows the modeled geology to be incorporated into physically based process models that are used to predict the behavior of geologic systems.   The 3D map also offers interesting new possibilities for visualizing complex geologic relations with the help of increasingly powerful computer software. Potential applications of the 3D map include:

1. Earthquake studies.

The intensity of earthquake shaking has been shown to depend strongly on the distribution of geologic units. For example, the intensity increases within sedimentary basins. Simulations of the shaking produced by the great 1906 San Francisco, California earthquake were based on a 3D velocity model made by assigning seismic velocities to the various rock units in a 3D geologic map of the San Francisco Bay region (see, for example, Hartzell and others, 2006; McPhee and others, 2007). Accurate seismic velocity models are required to precisely locate earthquake epicenters, which can be used to map fault location, geometry, and activity. A superior velocity model could be developed using the 3D geologic map that shows the regional distribution of geologic materials.

2. Ground water studies.

In urban areas, such as the San Francisco Bay region, ground water contamination from surface water pollution is a major problem (Howard, 1997). Because the flow of groundwater pollutants is governed by the porosity and permeability of materials, and these materials can often be related to

geologic units described in 3D geologic maps, contaminant flow and transport modeling can be improved by incorporating the subsurface distribution of the geologic units.

3. Mineral hazards studies.

Certain naturally occurring minerals can be hazardous to human health and the environment when disturbed by human development. Because certain minerals, such as asbestos and serpentinite, are associated with specific geologic units, geologic maps that show the subsurface distribution of those units can be used to regionally delineate the potential hazard.

4. Education and scientific inquiry.

A 3D geologic map allows the user to explore the shapes of the geologic units and structures, in isolation or as an integrated whole. Geologic features can be viewed from different angles, individually or in aggregate, and slices through the map can easily be constructed. This allows the user to grasp complex spatial relationships quickly and easily. Thus, 3D geologic maps are an excellent teaching aid and interpretive tool. This 3D map can be used by the academic community and by the public to understand the geology of the Hayward Fault at a regional scale.

Uses of this map database are limited by compilation scale and content, therefore the map is not intended for site-specific studies. Refer to the fault maps of the California Geological Survey (http://www.consrv.ca.gov/cgs/) for site-specific studies of fault activity.

Introduction

The Hayward Fault (fig. 1) is one of three major faults of the San Andreas Fault System that has produced large (M>6) historic earthquakes in the San Francisco Bay area; the other major faults are the San Andreas and Calaveras Faults. The Hayward Fault roughly bisects the San Francisco Bay area, a densely populated region of about seven million people. A severe earthquake, approximately M7 (U.S. Geological Survey, 2007), was generated by this fault zone in 1868, and a number of other major events have been captured in the paleoseismic record over the last 2,000 years (Lienkaemper and others, 2003). The Hayward-Rodgers Creek Fault zone (fig. 1) is considered to be the most likely source of a major earthquake in the San Francisco Bay area, with a probability of 27 percent for an earthquake ≥M6.7 over the next 30 years (Working Group on California Earthquake Probabilities, 2003). The Hayward Fault has the highest potential earthquake loss in the area due to the high concentration of manmade structures and lifelines in the region.

The purpose of this report is to describe the geology of the Hayward Fault zone and surrounding area and to provide views of the fault zone in three dimensions. The 3D geologic map is based on interpretations of geologic and geophysical data, modeling algorithms, and expert-driven decisions that were used to construct a geometric model of the inferred geology. The 3D map extends approximately 10 km on either side of the Hayward Fault, to a depth of 12 km.
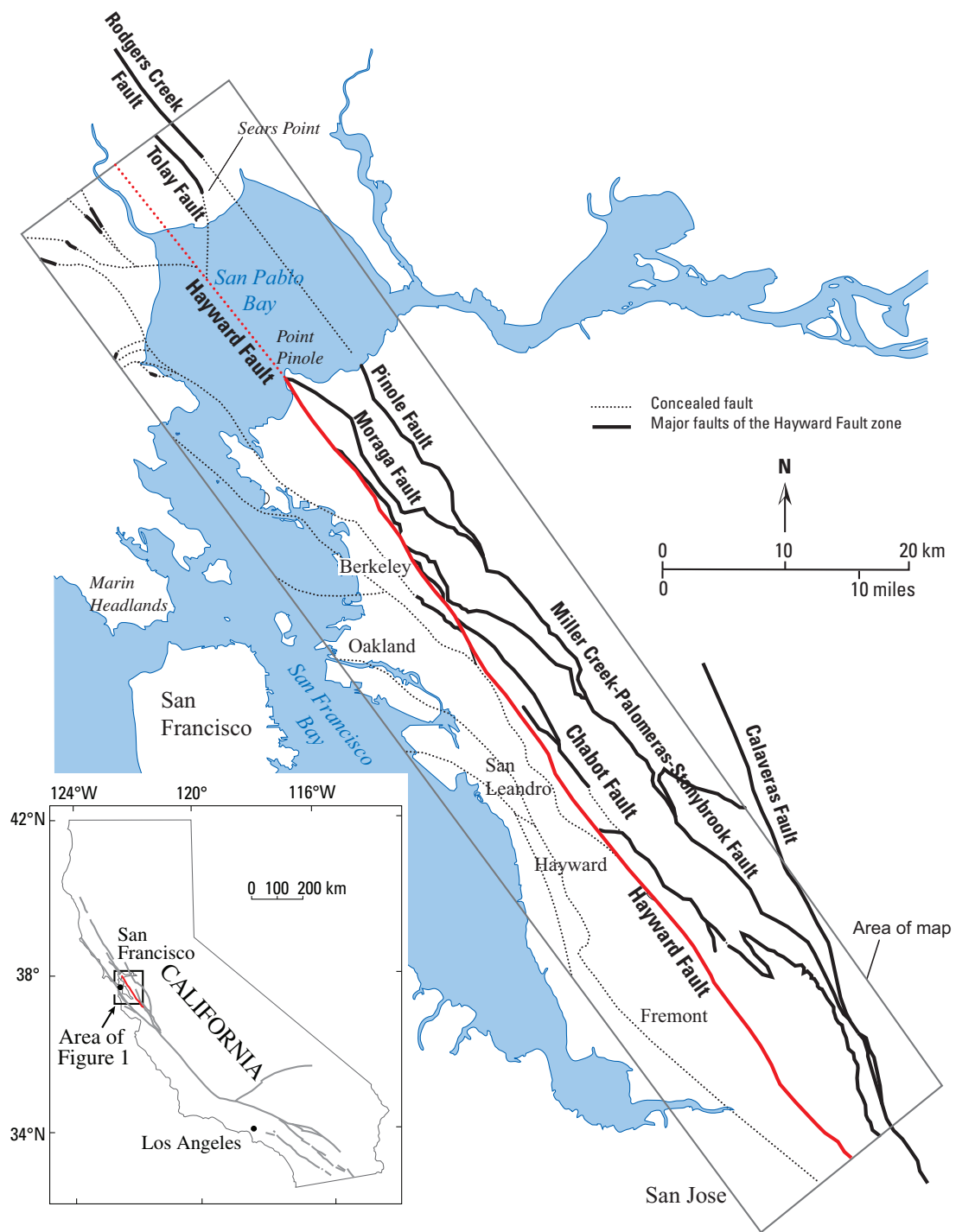
Figure 1. Generalized map of the major faults of the Hayward Fault zone (modified from Graymer and others, 2005).

The San Francisco Bay region includes nine counties surrounding San Francisco Bay and three major metropolitan areas: San Francisco, Oakland, and San Jose. The Hayward Fault demarcates the eastern side of the topographic San Francisco Bay plain; the East Bay hills extend along the east side of the fault (fig. 1). Within the map area, the metropolitan division of Oakland-Fremont-Hayward houses a population of approximately 2.5 million people (U.S. Census Bureau, 2006).

The map digital files are described in Appendix I. Instructions for viewing and querying the 3D geologic map are described in Appendix II.

Geologic Background

Mesozoic terrane complexes

A tectonostratigraphic terrane is a fault-bounded body of rock that has a geologic history that differs from those of adjacent rock bodies (Jones and others, 1983), implying some amount of displacement from its original position in order to juxtapose dissimilar rock bodies. Associated terranes (that is, terranes that share some common aspects of their geologic history) are grouped into terrane complexes. The Mesozoic rocks in the study area are composed of two terrane complexes (Blake and others, 1984; 2000; Graymer and others, 1996), the Franciscan Complex and the Great Valley complex (fig. 2). Each terrane complex comprises several related terranes (Blake and others, 1984).

The Great Valley complex is composed of at least five terranes, two of which crop out in the study area (the Healdsburg terrane and the Del Puerto terrane). Each terrane in the Great Valley complex is made up of Middle-Late Jurassic ophiolitic rocks (called collectively the Coast Range ophiolite), with or without Late Jurassic silicic volcanic rocks, and with one exception, is depositionally overlain by Late Jurassic and Cretaceous sedimentary strata (called cumulatively the Great Valley sequence). Although the origin of the Coast Range ophiolite remains controversial (see Dickinson and others [1996] for a summary of three different theories of Coast Range ophiolite origin), we herein accept the origin outlined in Graymer (2005) and Graymer and others (2006); the Coast Range ophiolite formed in the forearc of an oceanic island arc outboard of the North American continental margin, and the island arc and the forearc-related ophiolite were subsequently accreted to North America during the late Kimmeridgian Nevadan Orogeny (approximately 151-153 Ma). The earliest Great Valley sequence strata vary between terranes, but the bulk of Great Valley sequence sediments are thought to derive from a continental margin arc associated with the Sierra Nevada batholith (Ojakangas, 1968; Dickinson, 1970).

The Franciscan Complex is composed of many terranes, plus mélange (a chaotic mix of rocks derived from multiple terranes). In the study area, four coherent terranes (Yolla Bolly, Alcatraz Island, Marin Headlands, and Novato Quarry terranes), as well as mélange, crop out (Blake and others 1984; Graymer, 2000). Each coherent terrane in the Franciscan Complex is made up of one or more types of seafloor rocks (mid-ocean ridge basalt, seamount basalt, pelagic limestone and (or) chert, turbidite-derived sandstone and shale) accreted and amalgamated in a subduction zone (Ernst, 1969). The emplacement in the subduction zone has resulted in a low T/high P metamorphic overprint on some Franciscan Complex terranes ranging from incipient development of low T/high P minerals to complete metamorphism to glaucophane schist. Many Franciscan Complex terranes, however, have undergone only low-grade metamorphism, evidently not traveling deep into the subduction zone before being accreted to that overlying crust. For most of
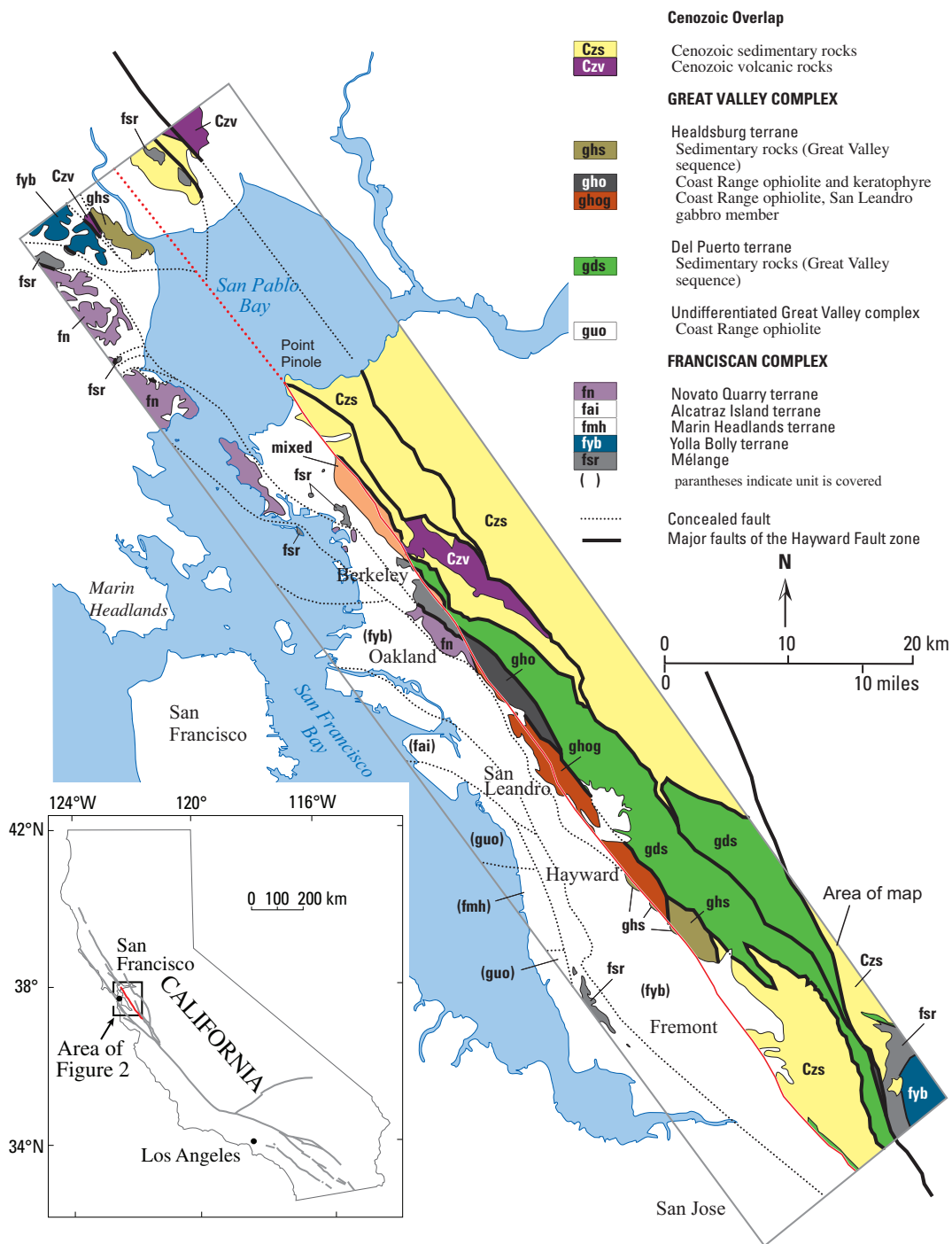
Figure 2. Generalized terrane map of the Hayward Fault zone (modified from Graymer and others, 2005).

the history of Franciscan accretion, the terranes have accumulated in the subduction zone's western margin of the North American Plate (a process that may be continuing today at the active Cascadia subduction margin to the north). However, Graymer (2005) showed that the age of the oldest Franciscan Complex metamorphic rocks suggest that these rocks were subducted into the trench associated with the island arc outboard of the North American subduction margin, and were carried to North America along with the island arc and forearc as described above.

The subduction emplacement of the Franciscan Complex means that Franciscan Complex terranes were originally all structurally under the Great Valley complex (although this position has been locally reversed by later tectonics as explained below). This juxtaposition allowed some admixture of materials of the two terrane complexes. Specifically, serpentinite from the base of the Coast Range ophiolite (Great Valley complex) is found entrained in the Franciscan Complex mélange, whereas high-grade metamorphic blocks (Franciscan Complex) are found entrained in serpentinite-matrix mélange that is associated with the Coast Range ophiolite. Previous workers have included serpentinite as a component of the Franciscan Complex, but the absence of middle-lower oceanic crust rocks in coherent Franciscan Complex terranes, as well as the plate tectonic model from Franciscan Complex terrane emplacement, suggests that the base of the downgoing (Franciscan Complex bearing) slab was entirely subducted, and that all serpentinite in the California Coast Ranges was originally part of the upper plate (Coast Range ophiolite). The emplacement of Franciscan Complex terranes beneath the Great Valley complex also implies that Franciscan Complex rocks exist at depth beneath exposed Great Valley complex rocks at least as far east as the Great Valley margin.

Paleogene unroofing and overlap

Although subduction and Franciscan Complex accretion at the western margin of the North American Plate continued into Neogene time, based on the presence of Miocene marine fossils in some Franciscan Complex terranes several hundred kilometers north of the study area (McLaughlin and others, 1996), accretion of the bulk of Franciscan Complex terranes was probably complete by about the end of the Cretaceous Period. Tectonic and(or) erosional unroofing of the Franciscan Complex terranes, as evidenced by the presence of Franciscan Complex detritus in Tertiary strata overlying Great Valley Sequence rocks, began in Paleocene time (Berkland, 1973) and was widespread by Eocene time (based both on the presence of Franciscan Complex detritus in Eocene strata and the presence of Eocene strata unconformably overlying Franciscan Complex rocks). Therefore, although certainly modified by later tectonics, the basic amalgamation of the two terrane complexes (Franciscan and Great Valley) was complete by Tertiary time. As a result, for this 3D map we treat all Tertiary strata in the San Francisco Bay region (except Tertiary Franciscan Complex terranes in northwestern Sonoma County) as an overlap sequence (that is, strata formed after amalgamation of separate terranes and deposited over both of the older units), even though the oldest units that are actually observed to be deposited on both terrane complexes are middle Miocene marine strata in the East Bay hills, the hills just east of the cities of Berkeley, Oakland, San Leandro, and Hayward (fig. 1) (Hall, 1958; Graymer and others, 1996).

Neogene transpression and development of the San Andreas Fault system

Starting about 30 Ma, the subduction zone at the western North American plate margin began to convert to the present transpressional margin during the formation and migration of two triple junctions, the Mendecino Triple Junction and the Baja Triple Junction (McKenzie and Morgan, 1969; Atwater, 1970; Atwater and Stock, 1988). In northern California this conversion resulted in

three major structural developments: the San Andreas Fault, a series of volcanic fields, and widespread compressive deformation. First, the largely strike-slip San Andreas Fault System was formed as the northwestward migrating Mendocino Triple Junction passed northern California. This system is made up of multiple faults, which jointly have accomodated at least 450 km of right-lateral offset over the past 23 m.y. (Matthews, 1976; Clark and others, 1984). In much of California about two-thirds of strike-slip offset has been taken up by the San Andreas Fault itself, but in the San Francisco Bay area, the fault system is complex and some strands of the presently active San Andreas Fault have taken up as little as 28 km of right-lateral slip (Cummings, 1968; Jachens and Zoback, 2000). About 175 km of the total strike-slip offset on the San Andreas Fault system has been taken up in the past 12 Ma by faults in the East Bay (Jones and Curtis, 1991; McLaughlin and others, 1996; Jachens and others, 1998), including about 100 km of offset on the Hayward Fault and about 50 km of offset on the Miller Creek-Moraga-Pinole Fault systems in the study area (Graymer and others, 2002a).

Second, in the wake of the migrating triple junction a northward-younging series of volcanic fields was developed (Fox and others, 1985). Many of these volcanic fields formed at or near the largely strike-slip faults of the San Andreas Fault System, and as a result parts of these volcanic fields have been widely separated; offset of correlated volcanic fields provide one of the primary controls on the amount and timing of fault offset.

Third, the late Neogene has been a time of widespread compressive deformation throughout the Coast Ranges (Suppe, 1977; Namson and Davis, 1984; Miller, 1999). Some of the compression has resulted from restraining bends and stepovers in the largely strike-slip faults (for example Andrews and others, 1993), but there is also a regional component of fault-normal compression as evidenced by 1) the uniformly compressed folded and reversely faulted Neogene strata in the region (Page, 1982), 2) a reverse-offset component of fault motion on some of the San Andreas Fault system, and 3) basement wedge-faulting (Wentworth and others, 1984; Unruh and Moores, 1992).

The results of the combined compressional and transform deformation in the San Francisco Bay region include two important developments. First, fault offset has juxtaposed structural blocks of differing stratigraphy (miniature terranes termed stratigraphic assemblages by Jones and Curtis, 1991). Second, during the Neogene, the present north-northwest trending ridges developed in the Coast Ranges (Dibblee, 1966; Vanderhurst and others, 1979; Jones and others, 1994; Graymer, 1995). The Berkeley-Oakland Hills in the study area were probably uplifted in Quaternary time, based on the presence of Pleistocene alluvial gravels near the ridge tops in the Oakland Hills, the hills just east of the city of Oakland (fig. 1) (Graymer, 2000).

Methods

The methods used to construct the 3D geologic map combined geologic mapping with geophysical mapping techniques. Geologic mapping techniques included the mapping of surface geology and inferring the sub-surface geology using down-dip projections and the surface geologic map patterns. Geophysical techniques were used to investigate the primarily unobservable subsurface. Geophysical techniques included seismic reflection and refraction surveys, tomography, and potential field surveys. Potential field surveys, especially gravity and magnetic data, which offered broad areal coverage, were used extensively to define geologic structures in this model (figs. 3 and 4). Several mapping techniques were applied in a complimentary fashion to maximize the effectiveness of each piece of evidence for different portions of the model; five areas in particular, the Hayward Fault, the east hills area (the hills just east of the cities of Berkeley, Oakland,

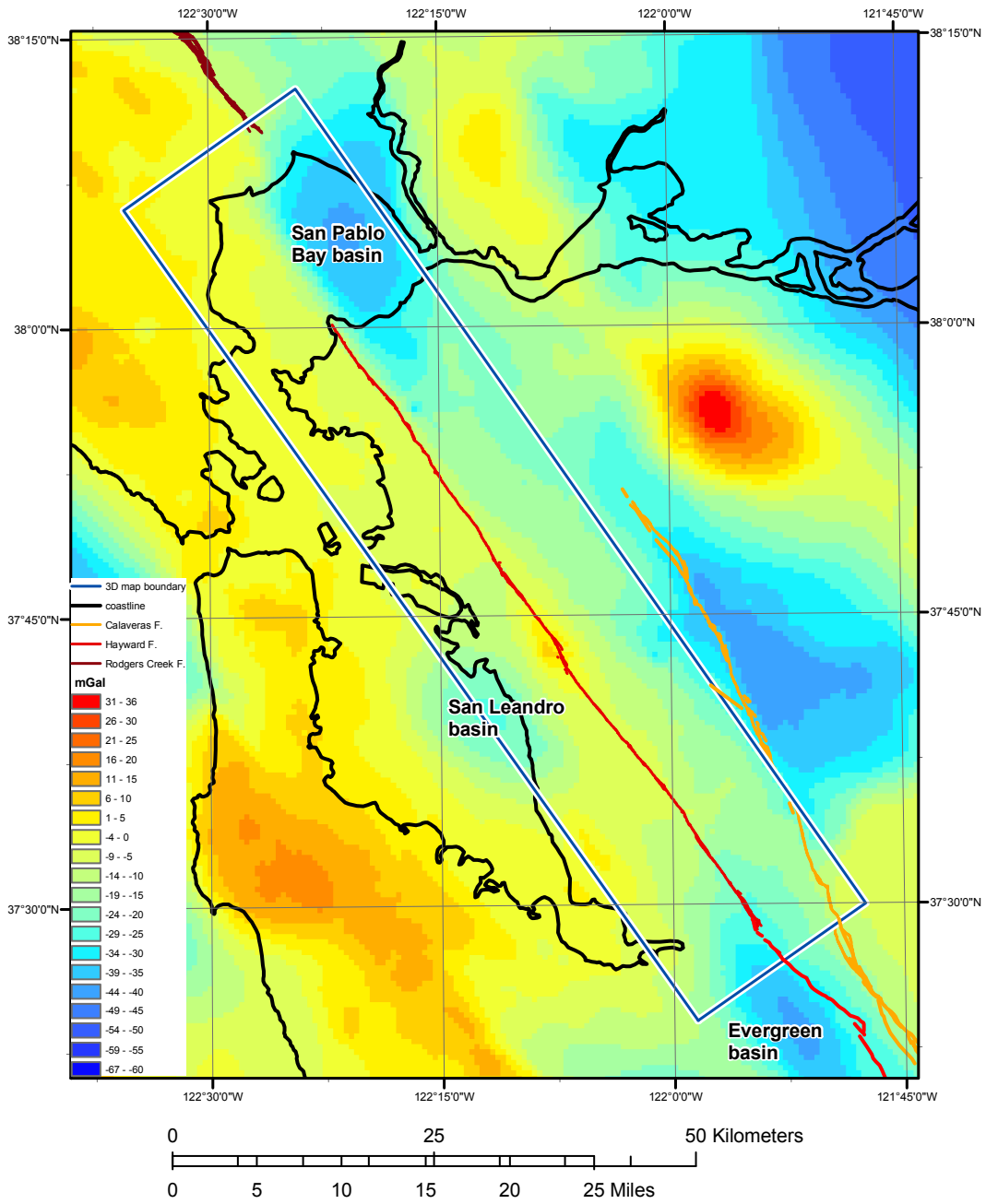**Figure 3**. Isostatic residual gravity anomaly map of the study area. Data from Roberts and Jachens (1993) and unpublished gravity data.
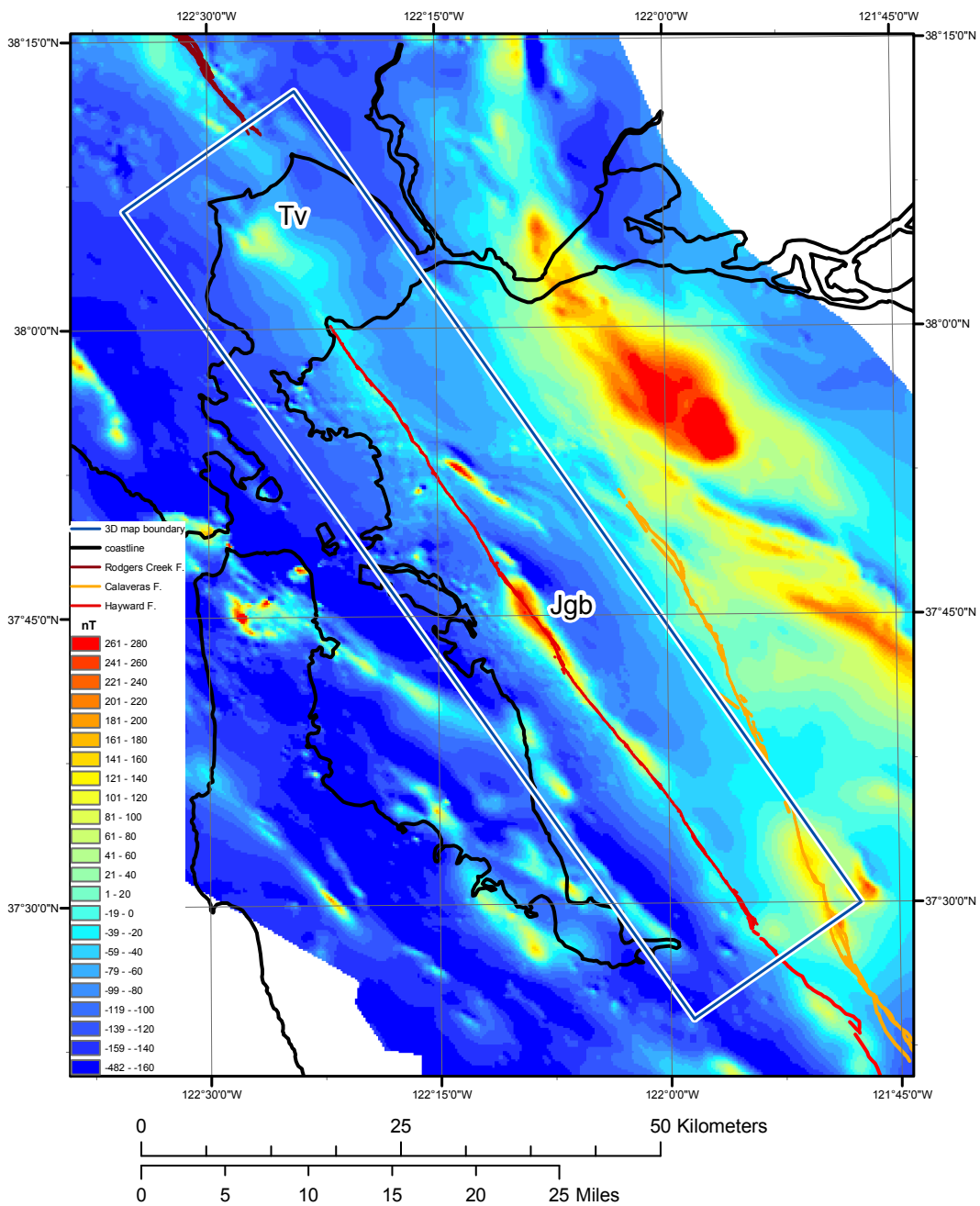
Figure 4. Magnetic anomaly map of the study area. Labels indicate the magnetic anomalies that helped define the volcanic rocks of uncertain age (Tv) and the rocks of the Coast Range ophiolite (Jgb). Data from U.S. Geological Survey (1999).

San Leandro, and Hayward, fig. 1), the Quaternary deposits and Tertiary volcanic deposits, the San Leandro gabbro of Ponce and others (2003), and the Mesozoic terranes west of the Hayward Fault, represent the full spectrum of mapping techniques used to make the 3D geologic map.

Hayward Fault

The Hayward Fault is represented in the map as a single surface, ignoring the possibility of multiple active strands in a finite width fault zone. This surface was created using two data sets: (1) the mapped trace of the creeping Hayward Fault (Lienkaemper, 1992), and (2) the locations of hypocenters of earthquakes from 1984-2000 relocated using the double-difference technique (Waldhauser and Ellsworth, 2000; Ponce and others, 2004). Software tools were used to project the fault trace onto the earth's surface, as defined by USGS 30-meter digital elevation models. Using map view slices spaced 1.25 km apart in depth, and cross-section slices perpendicular to the fault spaced 1.25 km apart along the fault, a set of curves, representing the fault trace in each profile, was constructed and adjusted by eye, honoring insofar as possible the surface fault trace data and the hypocenter data. Simpson and others (2003) show a set of sections at 2.5 km spacing, giving some impression of the hypocenter density along the fault. In places with few or no earthquakes, it was necessary to interpolate and extrapolate using the nearest clusters of events. When faced with ambiguities and complexities, our choice was to opt for a simple, smooth surface consistent with most hypocenters. In places where there were hints of multiple active strands, the surface was made to pass through either the better defined strand or the strand that resulted in a more continuous overall surface. Adjustments were made in an iterative fashion, alternating between map views and cross-section views, so that interpolations and extrapolations in both horizontal and vertical directions would be consistent. The curves were then sampled at 1.25 km intervals, to generate a set of xyz points. The final set of xyz points was then imported into EarthVision™ (Dynamic Graphics Inc.) to create the Hayward Fault surface using interpolation routines provided in the software. Additional control points were added as required, based on geologic reasoning, to remove artifacts created by the interpolation algorithm in areas of poor data control.

East Hills Area

East of the Hayward Fault, pre-Quaternary strata are exposed by the east-side-up component of motion within the fault zone. The strata are deformed; tight, complex folds and many minor faults result in a complicated geometry of faults and contacts. The fold patterns exposed at the surface and expressed on the surface geologic map aid in interpreting and representing the folds in three dimensions. The thickness of a unit in the stratigraphic sequence can be directly measured where both the upper and lower contacts are exposed. In addition, the inclination of the layers in an outcrop can be measured directly and are recorded as a strike and dip on a geologic map. Finally, the shape of subsurface folded layers can be inferred using a technique called down-plunge projection; the technique is based on the assumption that unit thickness is relatively constant, and that the shape of folded layers in the subsurface is proportional to the shape of the folded layers exposed at the surface.

We divided the volume east of the Hayward Fault into several smaller fault-bounded structural blocks in the East Hills region. Early attempts to create a 3D map ignored minor faults, and this effort failed because the amount of offset on a minor fault (less than 1 km of offset in map view) is in some cases greater than the grain of the structures and units in the map, resulting in unacceptable discontinuities. We modeled most of the minor faults as vertical because the mapped fault traces at the surface were generally undeflected by various slopes and valleys. However, one fault was

clearly nonvertical in outcrop, so we mapped it in the subsurface by assuming the downward projection of the estimated dip at the surface was constant along the length of the surface trace.

We then constructed the depositional contact surfaces according to the stratigraphy of each structural block. We drew a series of 1:24,000-scale cross sections using mapped contacts and strike and dip data from the surface geologic map, and estimated the depth to various depositional contacts at many points along the cross-section lines. We combined the cross sections to create a framework for drawing structure contour maps. The shape of the structure contours was manually interpolated between cross sections using the shape of the contact exposed at the surface and geologic interpretation of the structure. The structure contour maps formed the basis for the depositional surfaces in this region of the map.

Some depositional contacts in the 3D geologic map are not exposed at the surface within their structural block, but the statigraphy of the block indicates the contacts are probably present at depth. These subsurface geologic units in the 3D map were constructed by stacking layers of constant thickness below and parallel to the exposed units. The unit thickness was either measured within the same structural block or a representative unit thickness was derived from outcrops in adjacent blocks.

Two important assumptions are inherent in the technique described. First, we assumed a relatively constant unit thickness for stratified units unless there was surface map data to indicate a change in unit thickness. Because some stratified units in the mapped volume are known to change thickness, and even pinch out entirely, this is not always a good assumption. However, without data to suggest how stratified unit thickness changes in the subsurface, an assumption of constant thickness was used to project surface data into the subsurface. Second, we assumed that the stratified unit thickness observed in a small structural block defined by minor faults east of the Hayward Fault applies to unit thicknesses in adjacent small structural blocks. It seems likely that this assumption is better founded, because the unit thickness probably changes across a distance larger than the throw of the minor faults. Both assumptions could be tested in some cases. For example, if density contrasts permitted, a carefully constructed gravity model based on the depositional contacts predicted in the 3D geologic map could be compared with the observed gravity field, and the 3D map could be adjusted to better fit the gravity data.

Cenozoic sedimentary deposits and tertiary volcanic deposits

The thickness and subsurface extent of Cenozoic sedimentary deposits west of the Hayward Fault, including the northern end of the Evergreen Basin (fig. 3), were derived from the inversion of gravity data. In the vicinity of San Leandro the gravity data was coupled with limited offshore seismic reflection/refraction data (Marlow and others, 1999). The lower bounding surface of the Cenozoic layer represents the depositional unconformity between Cenozoic sedimentary and volcanic rocks (referred to in this text as basin deposits) and the underlying lower Tertiary and pre-Cenozoic rocks (referred to in this text as basement rocks) that consist of the Franciscan Complex west of the Hayward Fault and the Great Valley complex east of the Hayward Fault. The gravity inversion modeling process uses an estimated density contrast between the Cenozoic deposits and the Mesozoic rocks (Jachens and Moring, 1990). Estimated density increases (the density contrast decreases) with increasing depth (table 1). Through an iterative process the gravity anomaly is separated into two components: the gravity anomaly of the overlying basin deposits and the gravity anomaly of the basement rocks. The thickness of the basin deposits can then be calculated using the gravity anomaly associated with the basin component and the assumed density of the basin

deposits. Seismic reflection and refraction data, where available, can be used to cross-check the predicted depth of the basin deposits and constrain the estimated densities.

Table 1. Density-depth function for Cenozoic basin deposits and Cenozoic volcanic rocks used in the depth to basement process and relative to basement rocks (2670 kg/m^3)

Depth range (m)	Sedimentary rocks and sediments		Volcanic rocks	
	Contrast (kg/m^3)	Density (kg/m^3)	Contrast (kg/m^3)	Density (kg/m^3)
0-300	-550	2120	-450	2220
300-1300	-450	2220	-380	2290
1300-2300	-330	2340	-330	2340
2300-3300	-200	2470	-200	2470
> 3300	-100	2570	-100	2570

San Leandro gabbro of Ponce and others (2003)

The bounding surfaces of the San Leandro gabbro, which includes rocks of the San Leandro gabbro of Ponce and others (2003) and Coast Range ophiolite, were inferred from surface geologic mapping (Graymer and others, 1995), geophysical techniques such as boundary analysis (Blakely and Simpson, 1986), and 2-3/4 D gravity and magnetic modeling (Ponce and others, 2003).

These studies indicate the San Leandro gabbro of Ponce and others (2003) is approximately tabular in shape and oriented vertically, is about 25 km long, 3 km wide across the Hayward Fault, and extends at least 6-8 km depth. The Hayward Fault cuts through the gabbro body just east of its western edge, such that most of the gabbro is east of the Hayward Fault, but a narrow slice approximately 20 km long is west of the fault. The gabbro body dips about 75° NE in the vicinity of San Leandro. Farther to the south, the dip seems to decrease and the western edge of the gabbro body (west of the Hayward Fault) seems to merge with the Hayward Fault and to follow the subsurface trend of the seismicity associated with the fault. These data, plus independent constraints on the dip of the Hayward Fault, based on seismic reflection/refraction studies (Williams and others, 2005), combined with relocated seismicity data (Waldhauser and Ellsworth, 2002; Simpson and others, 2003; Ponce and others, 2004) suggest that the Hayward and Calaveras Faults may be connected at depths below about 5 km (Ponce and others, 2004; Manaker and others, 2005).

The lower bounding surface of the San Leandro gabbro west of the Hayward Fault was truncated against the fault at a depth of about 3 km, based on geophysical modeling that suggests the body dips into the fault here and is not deeper. This boundary also coincides with the depth extent of relocated seismicity data in this area (Graymer and others, 2005a). The gabbro west of the active trace of the Hayward Fault could represent a slice left behind in the fault zone, or could represent the westernmost of a series of anastomosing faults that comprise the Hayward Fault zone.

Geology west of the Hayward Fault

West of the Hayward Fault, within the map area, the Cenozoic section consists of Quaternary units that unconformably overlie Mesozoic basement rocks, except in the San Leandro basin and the Evergreen basin (fig. 3). Geologic relations mapped at the surface, and a number of drill holes logged during the building of public structures such as bridges and freeways, confirm that the Tertiary section has been removed from most of this portion of the map. The unconformity at the base of the Cenozoic section was mapped using gravity inversion modeling, as described in the

previous section. In the San Leandro basin (fig. 3) there is evidence for Tertiary deposits in the deeper parts of the basin. A seismic line (Marlow and others, 1999) across the basin shows an angular unconformity at the base of the Pleistocene, suggesting the Quaternary deposits overlie dipping, folded Tertiary deposits of uncertain affiliation.

The Mesozoic section west of the Hayward Fault consists primarily of terranes of the Franciscan Complex interleaved with tabular bodies of Coast Range ophiolite. These terranes and ophiolite bodies are exposed extensively in the Santa Cruz Mountains, east of the San Andreas Fault along the San Francisco Peninsula, and north of the Golden Gate bridge, tens of kilometers north and west of the map volume. However, close to the Hayward Fault the western Mesozoic section crops out in only a few places, and is otherwise covered by Cenozoic deposits. The Mesozoic units west of the Hayward Fault were mapped in the subsurface by defining the contacts between them at the Mesozoic bedrock surface and projecting these contacts to depth assuming a consistent dip normal to the strike of the near-surface contact. The contacts at the concealed bedrock surface were defined by examining the magnetic anomalies (fig. 3) that characterize bedrock where they crop out to the north and west, and following the anomalies into the subsurface. Geologic mapping (Blake and others, 2002) shows Mesozoic unit boundaries consistently dip approximately 65°eastward (Graymer and others, 2002b). On the basis of the geophysical anomalies, the terranes have a slab-like structure with an aspect ratio often exceeding 10:1 in map view; therefore, we projected the contacts between Mesozoic units to depth by assuming a constant eastward dip.

Description of Map Features

The choice of geologic units defined in this map is constrained by the ability to map the unit in three dimensions. In the structurally complex San Francisco Bay area, many geologic units shown in regional geologic maps (for example, Graymer and others, 2002b; Blake and others, 2000) are not included in the 3D map of the Hayward Fault because there is not sufficient data to map these units at depth.

Fault-bounded terranes and geologic units with a geophysical signature can form convenient mapping units when mapping in three dimensions; for example, the San Leandro gabbro of Ponce and others (2003) has a prominent associated magnetic anomaly (fig. 3). Units that crop out and that can be projected into the subsurface are mapped. Other units shown in detail on previously published 2D geologic maps are lumped into larger mappable units; for example, cherts of the Marin Headlands terrane of the Franciscan Complex are lumped with the Marin Headlands terrane unit, which is identified by its associated magnetic basalts. The Tertiary units in the 3D map have been significantly simplified from published 2D geologic maps. Furthermore, fault offset of units along the East Bay fault system has led to complex Tertiary stratigraphy that is not consistently reflected in the unit nomenclature. This is explained in detail in the Description of Map Units.

Several of the rock units are divided into sub-units, called "zones" in the map software, (for example, Fransiscan Complex mélange (unit **fsr)** has four sub-units: **fsr1**, **fsr2**, **fsr3, fsr4**). The number has no structural or stratigraphic significance but simply delineates geographic order, such as north to south.

Faults are modeled as single surfaces and are only generalizations of the fault zones in the map area because constructing a network of small surfaces over an entire fault zone is an intractable problem. We make the assumption that important features of the fault can be brought out with this simplified representation, generalizing by smoothing details that are difficult to model with the available data.

Only major faults that we considered important to regional geologic studies are represented; many faults that are mapped at the surface in previous publications are not included in the 3D map.

Description of Map Units

QTu   **Undivided Cenozoic sediments and sedimentary and volcanic rocks (Quaternary and Tertiary)** -- West of the Hayward Fault, unit consists of primarily Quaternary sediments, with the exception of Tertiary rocks in the San Leandro and Evergreen basins (fig. 3). East of the Hayward Fault, unit consists of deposits older than **Tus**, from Eocene to late Miocene in age. East of the Calaveras Fault, unit consists of Tertiary deposits. In San Pablo Bay, unit consists of Quaternary and Tertiary deposits younger than **Tv**

Tus   **Unnamed sedimentary and volcanic rocks (Tertiary)** -- Includes conglomerate, sandstone, siltstone, interbedded volcanics and limestone

Tv   **Volcanic rocks of uncertain age (Tertiary)** -- Defined solely by the presence of a large magnetic anomaly, interpreted as related to either the Berkeley Hills-Donnell Ranch volcanics (Graymer and others, 2002b; Youngman, 1989) or the western Sonoma volcanics (Graymer and others, 2002b) on the basis of the inferred continuity of the units based on the magnetic expression of the rocks

Tls   **Undivided sedimentary and volcanic rocks (Miocene and Eocene)** -- East of the Moraga Fault, consists of Tertiary units older than **QTu**. In San Pablo Bay, consists of Tertiary units older than **Tv**

Kfn   **Sandstone of the Novato Quarry terrane of Blake and others (1984) (Late Cretaceous)** -- Distinctly bedded to massive, fine- to coarse-grained, mica-bearing, lithic wacke. Where distinctly bedded, sandstone beds are about 1 m thick and siltstone interbeds are a few centimeters thick. Sedimentary structures are well preserved

Kfa   **Sandstone of the Alcatraz terrane of Blake and others (1984) (Cretaceous)** -- Coarse-grained, biotite- and shale-chip-bearing lithic wacke. Large biotite grains and shale chips up to 2 mm diameter are prominent in hand sample

KJfm   **Upper volcanic and sedimentary rocks of the Marin Headlands terrane of Blake and others (1984) (Cretaceous and Jurassic) --** Characterized by pillow basalt and diabase overlain by radiolarian chert and greywacke

fsr   **Franciscan Complex mélange (Early Cretaceous and/or Late Jurassic)** -- Sheared black argillite, graywacke, and minor green tuff, containing blocks and lenses of graywacke and metagraywacke, chert, shale, metachert, serpentinite, greenstone, amphibolite, tuff, eclogite, quartz schist, greenschist, basalt, marble, conglomerate, and glaucophane schist. Blocks range in size from pebbles to several hundred meters in length. East of the Calaveras Fault contains competent blocks of the Yolla Bolly terrane and Yolla Bolly greenstone (Graymer and others, 1996).

KJfy   **Metasandstone of the Yolla Bolly terrane of Blake and others (1982) (Early Cretaceous(?)and Late Jurassic)** -- Strongly foliated (textural zone 2 of Blake and others, 1967), coarse-grained, shale-chip-bearing lithic wacke. Jadeite characterizes the Yolla Bolly in this particular field area and jadite is visible under the hand lens and prominent in thin-section. Jadite indicates that the sandstone has been subjected to glaucophane schist metamorphism

KJfs **Franciscan Complex mélange (Early Cretaceous and/or Late Jurassic)** -- Massive to distinctly bedded siltstone, shale, and slate, grading into mélange consisting of sheared argillite and graywacke matrix enclosing blocks and lenses of sedimentary, metamorphic, and volcanic rocks (see unit **fsr** for a more complete description of mélange). Because contacts between coherent graywacke and mélange are gradational and because of the size and amount of cover in the map area, it was not possible in this study to differentiate everywhere between coherent graywacke and mélange. Coherent graywacke bodies also locally include conglomerate, pebbly sandstone, and rare thin beds of red and white chert

KJgvl **Great Valley Complex (Cretaceous and Late Jurassic)** -- Includes shale, conglomerate, sandstone, serpentinite and other ophiolitic rocks (as indicated by their magnetic expression) of Late Jurassic to Early Cretaceous age of the Healdsburg terrane

KJu **Undifferentiated Great Valley Complex rocks (Early Cretaceous and Late Jurassic)** -- Consists of sandstone, shale, conglomerate, and volcanic keratophyre and breccia

Jgb **Rocks of Coast Range ophiolite (Great Valley Complex) (Middle Jurassic) --** Here combined as the San Leandro gabbro. Consists mainly of gabbro, with minor faulted slivers of other mafic igneous rocks, keratophyre, and sedimentary rocks. Mafic rocks include pillow basalt, basalt breccia, minor diabase, and massive basalt and diabase. Also included are silicic igneous rocks from the Great Valley Complex: Late Jurassic keratophyre and quartz keratophyre, and shale with thin sandstone interbeds of the Cretaceous Knoxville Formation of the Great Valley Sequence. East of the Hayward Fault (zone **Jgb1** in the map), unit also includes minor Franciscan Complex mélange (**fsr**), mapped at the surface (Graymer, 2000), but here included in the generalized unit **Jgb**. The subsurface extent of **Jgb** is defined by geophysical modeling (Ponce and others, 2003).

Jo **Undifferentiated Coast Range Ophiolite of the Great Valley Complex (Middle Jurassic)** – Mostly serpentinite, with lesser serpentinite-matrix mélange, basalt, diabase, and gabbro. In the central part of the map volume, east of the Hayward Fault (zone **Jo2**), unit also includes altered Late Jurassic silicic and intermediate volcanics (quartz keratophyre and keratophyre), Early Cretaceous sandstone and shale (Great Valley Sequence) of the Healdsburg terrane, as well as minor fault-bounded slivers of Franciscan Complex mélange. In the north part of the map volume (zone **Jo1**), unit is rich in serpentinite-matrix mélange and has a significant component of infaulted slivers of Alcatraz Island and Yolla Bolly terranes of the Franciscan Complex, as well as mélange. The northern zone (zone **Jo1**) also includes minor amounts of Tertiary silicic volcanics (Murphy and others, 2002) and Great Valley Sequence of the Healdsburg terrane. West of the Hayward Fault, (zones **Jo3** and **Jo4**) consists of serpentinite

Description of Map Structures

Hayward Fault

The Hayward Fault is part of the Calaveras-Hayward-Rodgers Creek-Maacama-Healdsburg fault system. This fault system has experienced about 100 km of slip over the last 12 m.y. (Graymer and others, 2002a). While estimates of slip along the Hayward Fault have varied, recent published estimates indicate 65 km of slip on the Calaveras-Hayward-Rodgers Creek-Maacama-Healdsburg fault system, and 35 km of slip on the Calaveras-Hayward-Petaluma Valley fault system (Graymer, 2002a). The Holocene slip rate is estimated at approximately 9 mm/yr (Lienkaemper and

Borchardt, 1996). These two fault zones have accumulated twice as much slip as any other fault in the East Bay fault system, and almost three times as much slip in the past 6 Ma. The overall motion of the Hayward Fault is one of transpressional oblique-slip; reverse-slip accounts for approximately 10 percent of the motion. Interferometric synthetic aperture radar (InSAR) data (Bürgmann and others, 2000), a level-line survey (Gilmore, 1992), and uplift of Quaternary units (Kelson and Simpson, 1995; Graymer, 2000) all indicate a reverse component of slip on the fault. In the 3D map, the Hayward Fault is modeled as almost vertical through most of its length, but at the southeastern edge of the model, the fault begins to dip northeast as much as 60°. This change in fault dip is defined by the seismicity data and is consistent with geologic map relations in the field, where the surface expression of the fault has an east-dipping reverse component (Graymer and others, 1994).

Calaveras Fault

The Calaveras Fault extends from northeast of the study area (fig. 1) to the southern end of the San Francisco Bay region, south of Gilroy. Only 12 km of the northern section of the fault is in the map area. At the southern end of the Calaveras Fault, the fault has accumulated a total of about 160 km of right offset. Most of this offset propagated north onto a now concealed Proto-Calaveras Fault, and propagated through a releasing right-step onto the Hayward and Palomares-Miller Creek-Moraga-Pinole Faults (Graymer and others, 2002a; Graymer and others, 2005b). The right-step system was mostly abandoned about 2.5 Ma, when the currently active central Calaveras and northern Calaveras Faults formed (Graymer and others, 2005a; Graymer and others, 2005b). Currently most of the offset taken up by the central Calaveras Fault is transferred to the Hayward Fault through a restraining left-step (Andrews and others, 1993). The northern Calaveras (Sunol) Fault has probably accumulated only about 5 km of total offset (Graymer and others, 2002a). Only the south end of the northern Calaveras (Sunol) Fault, as defined by the Working Group on California Earthquake Probabilities (2003), is in the model, at the southernmost edge.

Rodgers Creek Fault

The Rodgers Creek Fault extends from San Pablo Bay approximately 40 miles northwest to the Santa Rosa area, where the fault connects to the Maacama Fault by way of a complex set of faults in the upper crust. Graymer and others (2002a) estimate that the Rodgers Creek Fault Zone, which may include proximal but presently inactive faults in addition to the active Rodgers Creek Fault, has accommodated approximately 45 km of right-lateral slip since about 10 Ma, based on correlation of the Berkeley Hills volcanics of Graymer and others (2002b) and the Donnell Ranch volcanics of Youngman (1989; see also Louderback, 1951; Fox and others, 1985; Curtis, 1989). Graymer and others (2002b) also estimate that 25 km of that right-lateral slip has accumulated since 3.5 Ma based on offset exposures of the Roblar Tuff (see also Sarna-Wojcicki, 1992) and other Sonoma Volcanics. The southernmost geomorphic expression of the Rodgers Creek Fault is north of San Pablo Bay near Sears Point, at the northwestern-most edge of the map volume. The fault is projected south and at depth into the map volume on the basis of analysis of a detailed gravity survey (Wright and Smith, 1992).

Palomares-Miller Creek-Moraga-Pinole Fault System

The Palomares-Miller Creek-Moraga-Pinole Fault system is roughly parallel to the Hayward Fault throughout the map area. The southern end of the fault system merges with the Calaveras Fault. The fault system has accommodated 50 km of total slip, all within the past 10 Ma. Thirty

kilometers of slip occurred between 10 and 6 Ma, and 20 km between 6 and 0 Ma. Therefore, between 10 and 6 Ma, the Palomares-Miller Creek-Moraga-Pinole Fault system was more active than the Hayward Fault, but currently it is not considered one of the active systems in the San Francisco Bay area.

The Palomares-Miller Creek-Moraga-Pinole Fault system is modeled as a single fault that extends from San Pablo Bay in the north to the Calaveras Fault in the south. In this map it is a transpressional fault system, assumed to be approximately parallel to the Hayward Fault. The surface trace was projected downward 60° to the west, a standard dip for reverse faults.

Chabot Fault

The Chabot Fault bounds the eastern edge of the San Leandro gabbro of Ponce and others (2003). There is no evidence of Holocene movement along this fault. The slip partitioned between the Hayward Fault and the Chabot Fault is unknown, but we estimate slip on the Chabot Fault is at least 25 km since about 3 Ma, based on the offset of the Irvington Gravel (Graymer and others, 1995).

Other San Leandro gabbro-bounding faults

The San Leandro gabbro is bounded by two subparallel faults that bifurcate and rejoin, forming a lens-shaped body. The eastern edge of the gabbro is bounded by the Chabot Fault; the western edge of the gabbro is bounded by an unnamed fault west of the Hayward Fault that merges with the Hayward Fault at a depth of about 5 km (Ponce and others, 2003).

Cretaceous/Tertiary (KT) faults east of the Hayward Fault

East of the Hayward Fault two faults form the eastern boundary of the block of Del Puerto terrane (of Blake and others, 1984) strata (fig. 2, unit **gds**). In the map volume the Del Puerto terrane is included as a subset of the unit **KJu**, and is not broken out. These two faults may be segments of a single fault intersected by the Moraga Fault system. The nature of the intersection is unclear; either the Moraga Fault system cuts and displaces the fault segments, or the fault segments are part of an intersecting system with contemporaneous movement. The Del Puerto terrane rocks are decoupled from the Tertiary rocks east of the Hayward Fault along faults, which are associated with deformation locally within the Tertiary section. East of the Hayward Fault the bedding is somewhat irregular and generally steeply dipping in both the Del Puerto terrane and the Tertiary units. Based on geologic mapping relations, the faults that separate Cretaceous and Tertiary strata were active between Miocene and very early Quaternary time.

San Pablo Bay Fault

The San Pablo Bay Fault, as shown in the map, is an amalgamation of the Tolay Fault, and the (informally named) San Pablo Bay Fault that truncates the unit **Tus** (unnamed Tertiary sedimentary and volcanic rocks) to form an edge of the basin underlying San Pablo Bay. The Tolay Fault is a thrust-fault mapped at the surface in the northern-most end of the map area. The Tolay Fault does not offset units younger than early Pleistocene (Hart, 1982); modern strike-slip movement occurs to the east on the Rodgers Creek Fault. The San Pablo Bay Fault is probably a normal fault associated with the pull-apart basin underlying San Pablo Bay in the strike-slip regime of the East Bay fault system. The trace of the San Pablo Bay Fault is mapped along the northwest margin of a magnetic anomaly that is inferred to represent an unbroken body of Tertiary basalt. The fault is roughly

collinear with northwest margin of the sedimentary basin as revealed by the negative gravity anomaly over the basin. Because the basin-bounding fault reflects extension in a releasing step, it is likely that the thrust offset of the Tolay Fault is superposed on (and obscures at the surface) the basin-bounding normal San Pablo Bay Fault in a manner similar to the Silver Creek Fault approximately 40 miles to the south (Graymer and others, 2005).

Cenozoic (Ce) faults east of the Hayward Fault

There are 13 Cenozoic faults east of the Hayward Fault (labeled Ce1 to Ce13) in the map. The Cenozoic faults cross-cut topography, indicating that their dip is approximately vertical, and were modeled as such. Though the faults have been mapped on published geologic maps, they have not been named. We name them with the prefix Ce, *Cenozoic* faults *east* of the Hayward Fault, and a number from 1 to 13, approximately north to south. In general, these faults are Pliocene or younger and offset Tertiary units in the northern part of the map area east of the Hayward Fault. Typical offsets are 1 km or less. The faults are associated with folding in the Tertiary units. The order of faulting was determined by cross-cutting relations portrayed on the geologic maps (Graymer, 2000).

These faults do not have significant offset in a regional sense, and would have been left out of the map in the generalization process had it not been for a technical difficulty. The Cenozoic deposits that these faults cut could not be modeled without including the faults. The bedding planes that bound the Cenozoic deposits were modeled by interpolating scattered data to form a surface. However, the faults caused differences in elevation among the scattered data points, which prevented the spline algorithm from smoothly interpolating between the data points. As a result, the algorithm became unstable and generated high-amplitude waveforms between the offsets. By adding the faults to the map, scattered data from one side of a fault are automatically separated from scattered data on the opposite side of the fault. Therefore, including the faults in the map allowed the algorithm to smoothly interpolate between the scattered data and to generate smooth bedding surfaces. Although the offset along the Cenozoic faults east of the Hayward Fault is minor compared to the general resolution of the map, including the faults in the map resulted in a more accurate depiction of the geology.

Mesozoic (Mw) faults west of the Hayward Fault

There are 11 Mesozoic faults west of the Hayward Fault (labeled Mw1 to Mw11) in the map. We name them with the prefix Mw, *Mesozoic* faults *west* of the Hayward Fault, and a number from 1 to 11, approximately north to south. These faults are entirely overlain by Cenozoic, primarily Quaternary, deposits, and the faults and fault geometry is not based on direct observation, but is inferred from the sparsely exposed terranes of the Franciscan Complex, which are known to be fault-bounded based on exposures elsewhere in the San Francisco Bay area. The location of the faults was inferred from potential-field data, primarily aeromagnetic anomalies (fig. 3). The fault traces, determined from the geophysical maps, were given a constant dip of 60° east, based on the dip of analogous faults that bound terranes in the Franciscan Complex in the northern San Francisco Bay area (Blake and others, 2000; Blake and others, 2002; Graymer and others, 2002b). The order of faulting was determined by the cross-cutting relations of the fault traces.

Data

Explanations of the data and algorithms used to construct the 3D geologic map features are contained in table 2.

Table 2. Description of data and algorithms

STRUCTURAL FEATURE NAME	Technical methods used to generate 3D geometry
Hayward Fault	Fault was constructed based on data from surface geology and earthquake hypocenters. Mapped trace taken from the following geologic maps: Lienkamper, 1992; Graymer and others, 1996; Graymer, 2002b. Earthquake hypocenters from Waldhauser and Ellsworth (2002). Earthquake hypocenters, viewed in vertical cross-sections at regularly spaced intervals along the fault, were used to define the Hayward Fault surface, as discussed in the Methods section. The EarthVision 3D griding algorithm was used to generate the curved surface of the Hayward Fault. Control points were added to constrain regions where the interpolation algorithm became unstable and generated spurious results.
Calaveras Fault	Trace and dip of the Calaveras Fault was based on surface geologic mapping (ref) and seismicity (Waldhauser and Ellsworth, 2000). The surface trace was digitized at intervals fine enough to capture the desired level of detail. A surface was fit to the data points described by the surface trace of the fault and the seismicity using a bi-cubic spline algorithm (Briggs, 1974).
Rodgers Creek Fault	Trace and dip of the Rodgers Creek Fault based on analysis of gravity anomalies and drill hole data beneath San Pablo Bay (Wright and Smith, 1992). Data was digitized from the report; the trace of the fault at the surface was discretized into a series of points. For most of its length the fault is modeled as a vertical fault, and the surface trace projected vertically through the model to generate the fault surface. At the very southern end the fault was modeled as dipping to the northeast, based on seismic data from Wright and Smith (1992). The algorithm used in constructing this northeastern-dipping section (DeKemp, 1998) extrapolated the trace of the faults down-dip at an angle of 80 degrees (based on Wright and Smith [1992]).

Palomares-Miller Creek-Moraga-Pinole Fault, Chabot Fault, Jgb west-bounding fault

The traces of these faults were taken from geologic maps (Graymer, 2000) and digitized at intervals fine enough to capture the desired level of detail. The algorithm used in constructing the faults (DeKemp, 1998) extrapolated the trace of the faults down-dip at a given angle. The angle chosen was based on an angle of 60º W, typical of reverse faults.

Other San Leandro gabbro-bounding faults

The western boundary of the San Leandro gabbro, west of the Hayward Fault, merged two types of data to generate the fault surface: surface geology and geophysical modeling. The mapped surface trace of the fault (Graymer, 2000) was discretized into a series of points in space and projected downward and truncated at depth, based on gravity and magnetic modeling that suggests the gabbro body dips into the fault here and is not deeper than about 3 km (Ponce and others, 2003). The software used to perform the gravity magnetic modeling was GMSYS (Northwest Geophysical Associates, Inc.). Details of the modeling are discussed in Ponce and others (2003).

KT faults

The traces of these faults were taken from geologic maps (Graymer and others, 1996; Graymer and others, 1994) and digitized. The traces were extrapolated down-dip at an angle of 60º, typical of reverse faults.

San Pablo Bay Fault

The San Pablo Bay Fault represented here is an amalgamation of the mapped Tolay Fault and the (informally named) San Pablo Bay Fault that strikes northeast and merges with the Hayward Fault. The surface trace of the Tolay Fault was digitized from geologic map data (Wentworth, 1997), and the surface trace of the San Pablo Bay Fault was inferred from analysis of the gradient of the gravitational field digitized from gravity anomaly data (Wright and Smith, 1992). The trace of the faults at the surface was discretized into a series of points located in space. The trace of the faults was extrapolated (using the algorithm by DeKemp, 1998) down-dip 79 degrees for the mapped Tolay portion of the fault (based on cross sections published in Wright and Smith (1992)). The dip of the San Pablo Bay Fault to the south was assumed to be vertical. The data for both faults was merged into one fault trace prior to extrapolation.

Cenozoic East faults

Mapped trace as shown on surface geologic maps (Graymer, 2000), Surface fault trace was discretized into a series of points located in space, and the points projected vertically downward at discrete intervals to form a vertical "curtain" of points. This was then gridded in three dimensions using the algorithms within the EarthVision software.

Mesozoic west faults

Indirect data was used to construct these faults. The trace of these faults in the subsurface was defined by the local maximum horizontal gradient of geophysical anomalies (figs. 2 and 3). The traces were projected onto the modeled surface of the bottom of the Cenozoic section. The algorithm used in constructing the faults (DeKemp, 1998) extrapolated the trace of the faults down-dip at a given angle. The angle chosen was based on observed outcrop relationships outside the study area.

Base of the Cenozoic section

Gravity data (fig. 3; Roberts and Jachens, 1993) was used as the primary data source to construct the base of the Cenozoic section (see Methods section). The results were compared with limited seismic data for the San Leandro basin (Marlowe and others, 1999). The gravity data were interpolated using a bi-cubic spline algorithm (Briggs, 1974) and modeled using the iterative inverse modeling technique developed by Jachens and Moring (1990; see Methods section).

Paleogene basal contact

The Paleogene basal contact that occurs east of the Hayward Fault and in the map was projected into the model based on observations to the northeast, in Contra Costa County (Graymer and others, 1994). The basal contact was mapped assuming constant thickness of the Tertiary section projected downward from the surface.

Tertiary volcanic rocks of uncertain age

Magnetic data (fig. 4; U.S. Geological Survey, 1999) was used to generate the Tertiary volcanic unit. The magnetic data were collected along flight lines with 500 meter spacing at a nominal height of 300 meters above ground. The data have a resolution of approximately 100 meters parallel to flight lines and 500 meters perpendicular to flight lines. The edges of the volcanic body in the map view were determined from its magnetic anomaly following the method of Blakely and Simpson (1986). The depth and thickness of the body were determined by forward modeling of the magnetic anomaly, constrained by drill hole information and seismic reflection profile interpretations (Wright and Smith, 1992; Smith, 1992).

Acknowledgments

References Cited

Aagaard, B.T., 2006, Finite-element simulations of ground motions in the San Francisco Bay area from large earthquakes on the San Andreas Fault: Seismological Research Letters, v. 77, p. 275.

Andrews, D.J., Oppenheimer, D.H., and Lienkaemper, J.J., 1993, The Mission link between the Hayward and Calaveras Faults: Journal of Geophysical Research, v. 98, no. B7, p. 12,083-12,095.

Argus, D.F., and Gordon, R.G., 2001, Present tectonic motion across the Coast Ranges and San Andreas Fault system in central California: Geological Society of America Bulletin, v. 113, no.12, p. 1,580-1,592.

Atwater, Tanya, 1970, Implications of plate tectonics for the Cenozoic tectonic evolution of western North America: Geological Society of America Bulletin, v. 81, p. 3,513-3,536.

Atwater, T. and Stock, J., 1998, Pacific-North America plate tectonics of the Neogene southwestern United States - An Update: International Geological Review, v. 40, p. 375-402.

Barrall, M., and Simpson, R., 2006, A high-resolution finite element model of the Hayward Fault: Third Annual Northern California Earthquake Hazards workshop, January 18-19, 2006, p. 20-21.

Bartow, J.A., 1985, Map and cross sections showing Tertiary stratigraphy and structure of the northern San Joaquin Valley, California: U.S. Geological Survey Miscellaneous Field Studies Map MF-1761, scale 1:250,000.

Berkland, J.O., 1973, Rice Valley outlier—new sequence of Cretaceous-Paleocene strata in northern Coast Ranges, California: Geological Society of America Bulletin 84, p. 2,389-2,406.

Beyer, L.A., 1980, Borehole gravity program of the U.S. Geological Survey (1963-1975)—Brief history and basic data: U.S. Geological Survey Open-File Report 80-903, 76 p.

Blake, M.C. Jr., Graymer, R.W., and Jones, D.L., 2000, Geologic map and map database of parts of Marin, San Francisco, Alameda, Contra Costa, and Sonoma Counties, California: U.S. Geological Survey Miscellaneous Field Studies MF 2337, 31 p., scale 1:75,000 [http://pubs.usgs.gov/mf/2000/2337/].

Blake, M.C. Jr., Graymer, R.W., and Stamski, R.E., 2002, Geologic map and map database of western Sonoma, northernmost Marin, and southernmost Mendocino Counties, California: U.S. Geological Survey Miscellaneous Field Studies MF 2402, 43 p., scale 1:62,500 [http://pubs.usgs.gov/mf/2002/2402/].

Blake, M.C., Jr., Howell, D.G., and Jayko, A.S., 1984, Tectonostratigraphic terranes of the San Francisco Bay region, *in* Blake, M.C., ed., 1984, Franciscan Geology of northern California: Pacific Section, Society of Economic paleontologists and mineralogists, v. 43, p. 5-22.

Blake, M.C., Jr., Howell, D.G., and Jones, D.L., 1982, Preliminary tectonostratigraphic terrane map of California: U.S. Geological Survey Open-File Report 82-593, 9 p., 3 maps, scale 1:750,000 [http://pubs.er.usgs.gov/usgspubs/ofr/ofr82593].

Blake, M.C., Jr., Irwin, W.P., and Coleman, R.G., 1967, Upside-down metamorphic zonation, blueschist facies, along a regional thrust in California and Oregon: U. S. Geological Survey Professional Paper 575C, p. 1-9.

Blakely, R.J., and Simpson, R.W., 1986, Approximating edges of source bodies from magnetic or gravity anomalies: Geophysics, v. 51, p. 1,494-1,496.

Briggs, I., 1974, Machine contouring using minimum curvature: Geophysics, v. 39, no. 1, p. 39–48.

Brocher, T.M., 2005, A regional view of urban sedimentary basins in northern California based on oil industry compressional-wave velocity and density logs: Bulletin of the Seismological Society of America, v. 95, no. 6, p. 2,093-2,114.

Bürgmann, R., Schmidt, D., Nadeau, R.M., d'Alessio, M., Fielding, E., Manaker, D., McEvilly, T. V., and Murray, M.H., 2000, Earthquake potential along the northern Hayward Fault, California: Science, v. 289, no. 5482, p. 1,178-1,182.

Clark, J.C., Brabb, E.E, Greene, H.G., Ross, D.C., 1984, Geology of Point Reyes Peninsula and implications for San Gregorio Fault history: Field Trip Guidebook - Pacific Section, Society of Economic Paleontologists and Mineralogists, v. 38, p. 67-85.

Cummings, J.C., 1968, The Santa Clara Formation and possible post-Pliocene slip on the San Andreas Fault in central California: Stanford University Publications, Geological Sciences, v. 11, p. 191-206.

Curtis, G.H., 1989, Berkeley Hills *in* Wahrhaftig, C., ed., Geology of San Francisco and vicinity, 28th International Geological Congress Field Trip Guidebook T105: American Geophysical Union, Washington, D.C., p. 47-52.

De Kemp, E.A., 1998, Three-dimensional projection of curvilinear geological features through direction cosine interpolation of structural field observations: Computers & Geosciences, v. 24, no. 3, p. 269-284.

Dibblee, T.W., Jr., 1966, Evidence for cumulative offset on the San Andreas Fault in central and northern California: California, Division of Mines and Geology Bulletin, v. 190, p. 375-384.

Dickinson, W.R., 1970, Tectonic setting and sedimentary petrology of the Great Valley sequence: Geological Society of America Abstracts with Programs, v. 2, no. 2, p. 86-87.

Dickinson, W.R., Hopson, C.A. Saleeby, J.B., Schweickert, R.A., Ingersoll, R.V., Pessagno, E.A., Jr, Mattinson, J.M., Luyendyk, B.P., Beebe, W., Hull, D.M., Munoz, I.M., and Blome, C.D., 1996, Alternate origins of the Coast Range ophiolite (California); introduction and implications: GSA Today, v. 6, no. 2, p. 1-10.

Ernst, W.G., 1969, Tectonic contact between the Franciscan mélange and the Great Valley sequence, a late Mesozoic Benioff zone: Geological Society of America, Annual Meeting Abstracts, Part 7, p. 59.

Fox, K.F., Jr., Fleck, R.J., Curtis, G.H., and Meyer, C.E., 1985, Implications of the northwestwardly younger age of the volcanic rocks of west central California: Geological Society of America Bulletin, v. 96, p. 647–654.

Gilmore, T.D., 1992, Historical uplift measured across the eastern San Francisco Bay region, *in* Borchardt, G., and others, eds., Proceedings of the Second Conference on Earthquake Hazards in the Eastern San Francisco Bay area: California Division of Mines and Geology Special Publication 113, p. 55–62.

Graymer, R.W., 1995, Geology of the Southeast San Francisco Bay area hills, California: Society of Economic Paleontologists and Mineralogists—Pacific Section, v. 76, p. 115-124.

Graymer, R.W., 2000, Geologic map and map database of the Oakland metropolitan area, Alameda, Contra Costa, and San Francisco Counties, California: U.S. Geological Survey Miscellaneous Field Studies Map MF-2342, 29 p., scale 1:50,000 [http://pubs.usgs.gov/mf/2000/2342/].

Graymer, R.W., 2005, Jurassic-Cretaceous assembly of central California, *in* Stevens, Calvin, and Cooper, John, eds., Mesozoic tectonic assembly of California: Pacific Section, Society of Economic Paleontologists and Mineralogists Book 96, p. 21-64.

Graymer, R.W., Jones, D.L., and Brabb, E.E., 1994, Preliminary geologic map emphasizing bedrock formations in Contra Costa County, California; A digital database: U.S. Geological Survey Open-File Report 94-622. [http://pubs.usgs.gov/of/1994/of94-622/]

Graymer, R.W., Jones, D.L., and Brabb, E.E., 1995, Geologic map of the Hayward Fault zone, Contra Costa, Alameda, and Santa Clara Counties, California; A digital database: U.S. Geological Survey Open-File Report 95-597, includes plotfiles for 3 sheets, scale 1:50,000, database description pamphlet, 9 p., geologic description and interpretation pamphlet, 16 p. [http://pubs.usgs.gov/of/of95-957]

Graymer, R.W., Jones, D.L., and Brabb, E.E., 1996, Preliminary geologic map emphasizing bedrock formations in Alameda County, California; A digital database: U.S. Geological Survey Open-File Report 96-252, 33 p., scale 1:75,000. [http://pubs.usgs.gov/of/1996/of96-252/]

Graymer, R.W., Jones, D.L., and Brabb, E.E., 2002b, Geologic map and map database of northeastern San Francisco Bay region, California: U.S. Geological Survey Miscellaneous Field Studies Map MF-2403, 30 p., scale 1:62,500. [http://pubs.usgs.gov/mf/2002/2403/]

Graymer, R.W., Sarna-Wojcicki, A.M., Walker, J.P., McLaughlin, R.J., and Fleck, R.J., 2002a, Controls on timing and amount of right-lateral offset on the East Bay fault system, San Francisco Bay region, California: Geological Society of America Bulletin, v. 114, no. 12, p. 1,471-1,479.

Graymer, R.W., Ponce, D.A., Jachens, R.C., Simpson, R.W., and Wentworth, C.M., 2005a, 3D geologic map of the Hayward Fault, northern California; correlation of rock units with variations in seismicity, creep rate, and fault dip: Geology, v. 33, no. 6, p. 521-524, doi:10.1130/G21435.1, 4 p.

Graymer, R.W., McLaughlin, R.J., Stanley, R.G., Ponce, D.A., Jachens, R.C., Simpson, R.W., and Wentworth, C.M., 2005b, Santa Clara Valley-bounding faults characterized by structural superposition: Geological Society of America Abstracts with Programs, v. 37, no. 4, p. 58.

Graymer, R.W., Moring, B.C., Saucedo, G.J., Wentworth, C.M., Brabb, E.E., and Knudsen, K.L., 2006, Geologic map of the San Francisco Bay region: U.S. Geological Survey Scientific Investigations Map 2918, scale 1:275,000 [http://pubs.usgs.gov/sim/2006/2918/].

Graymer, R.W., Langenheim, V.E., Simpson, R.W., Jachens, R.C., and Ponce, D.A., 2008, Relatively simple through-going fault planes at large earthquake depth may be concealed by surface complexity in stepover regions, *in* Mann, Paul, and Cunningham, Dickson, eds., Tectonics of strike-slip restraining and releasing bends in continental and oceanic settings: Geological Society of London Special Volume 290, Geological Society of London, 488 p.

Hall, C.A., Jr., 1958, Geology and paleontology of the Pleasanton area, Alameda and Contra Costa counties, California: University of California Publications in Geological Sciences, v. 34, no. 1, p. 1-89.

Hart, E.W., 1982, Tolay Fault; Sears Point, Petaluma River, Glen Ellen, Cotati, and Two Rock 7.5-minute quadrangles, California: California Division of Mines and Geology Fault Evaluation Report FER-140, 13 p., scale 1:24,000.

Hartzell, S., Harmsen, S., Williams, R.A., Carver, D., Frankel, A., Choy, G., Liu, P.C., Jachens, R.C., Brocher, T.M., and Wentworth, C.M., 2006, Modeling and validation of a 3D velocity structure for the Santa Clara Valley, California, for seismic-wave simulations: Bulletin of the Seismological Society of America, v. 96, no. 5, p. 1,851-1,881.

Howard, K.W.F., 1997, Impacts of urban development on groundwater *in* Eyles, Nicholas, ed., Environmental geology of urban areas: Geological Association of Canada Geotext 3, p. 93-104.

Irwin, W.P., 1990, Geology and plate-tectonic development, *in* Wallace, R.E., ed., The San Andreas Fault System, California: U.S. Geological Survey Professional Paper 1515, p. 61-80 [http://pubs.usgs.gov/pp/1990/1515/].

Jachens, R.C., and Moring, B.C., 1990, Maps of the thickness of Cenozoic deposits and the isostatic residual gravity over basement for Nevada: U.S. Geological Survey Open-File Report 90-404, 15 p. [http://pubs.er.usgs.gov/usgspubs/ofr/ofr90404].

Jachens, R.C., Wentworth, C.M., and McLaughlin, R.J., 1998, Pre-San Andreas location of the Gualala Block inferred from magnetic and gravity anomalies: Pacific Section, Society of Economic Paleontologists and Mineralogists, v. 84, p. 27-63.

Jachens, R.C., Wentworth, C.M., McLaughlin, R.J., and Graymer, R.W., 2006, Geophysical piercing 'features' defining offset in the San Andreas Fault system, northern California: Seismological Research Letters, v. 77, p. 200.

Jachens, R.C., and Zoback, M.L., 2000, The San Andreas Fault in the San Francisco Bay region, California; structure and kinematics of a young plate boundary: International Book Series, v. 3, p. 217-231.

Jones, D.L., Howell, D.G., Coney, P.J., Monger, J.W.H., 1983, Recognition, character and analysis of tectonostratigraphic terranes in western North America: Journal of Geological Education, v. 31, no. 4, p. 295-303.

Jones, D.L., and Curtis, G.H., 1991, Guide to the geology of the Berkeley Hills, central Coast Ranges, California, *in* Sloan, Doris, and Wagner, D.L., eds., Geologic excursions in northern California; San Francisco to the Sierra Nevada: California Division of Mines and Geology Special Publication 109, p. 63-74.

Jones, D.L., Graymer, R.W., Wang, C., McEvilly, T.V., and Lomax, A., 1994, Neogene transpressive evolution of the California Coast Ranges: Tectonics, v. 13, no. 3, p. 561-574.

Kelson, K.I., and Simpson, G.D., 1995, Late Quaternary deformation of the southern East Bay Hills, Alameda County, California: American Association of Petroleum Geologists Bulletin, v. 79, p. 590.

Lienkaemper, J.J., 1992, Map of recently active traces of the Hayward Fault, Alameda and Contra Costa Counties, California: U.S. Geological Survey Miscellaneous Map MF-2196, 13 p., scale 1:24,000 [http://pubs.usgs.gov/mf/1992/2196/].

Lienkaemper, J.J, Borchardt, G., 1996, Holocene slip rate of the Hayward Fault at Union City, California: Journal of Geophysical Research, v. 101, no. B3, p. 6,099-6,108.

Lienkaemper, J.J., Williams, P.L., Dawson, T.E., Personius, S.F., Seitz, G.G., Heller, S.J., and Schwartz, D.P., 2003, Logs and data from trenches across the Hayward Fault at Tyson's Lagoon (Tule Pond), Fremont, Alameda County, California, 2001-2003: U.S. Geological Survey Open-File Report 03-488, version 3.0, 5 p. [http://pubs.usgs.gov/of/2003/of03-488/].

Louderback, G.D., 1951, Geologic history of San Francisco Bay, *in* Jenkins, O.P., ed., Geologic guidebook of the San Francisco Bay counties: California Division of Mines and Geology Bulletin 154, p. 75-94.

Manaker, D.M., Michael, A., and Bürgmann, R., 2005, Subsurface structure and kinematics of the Calaveras-Hayward Fault stepover from 3D Vp and seismicity, San Francisco Bay region, California: Bulletin of the Seismological Society of America, v. 95, no. 2, p. 446-470.

Marlow, M.S., Jachens, R.C., Hart, P.E., Carlson, P.R., Anima, R.J., and Childs, J.R., 1999, Development of San Leandro synform and neotectonics of the San Francisco Bay block, California: Marine and Petroleum Geology, v. 16, p. 431-442.

Matthews, V., 1976, Correlation of Pinnacles and Neenach Volcanic formations and their bearing on San Andreas Fault problems: American Association of Petroleum Geologists Bulletin, v. 60, no. 12, p. 2,128-2,141.

McKenzie, D.P., and Morgan, W.J., 1969, Evolution of triple junctions: Nature, v. 224, no. 5215, p. 125-133.

McLaughlin, R.J., Kling, S.A., Poore, R.Z., McDougall, Kristin, and Beutner, E.C., 1982, Post-middle Miocene accretion of Franciscan rocks, northwestern California: Geological Society of America Bulletin, v. 39, no. 7, p. 595-605.

McLaughlin, R.J., Sliter, W.V., Sorg, D.H., Russell, P.C., and Sarna-Wojcicki, A.M., 1996, Large-scale right-slip displacement on the east San Francisco Bay region fault system, California; implications for location of late Miocene to Pliocene Pacific Plate boundary: Tectonics, v. 15, no. 1, p. 1-18.

McPhee, D.K., Langenheim, V.E., Hartzell, S., McLaughlin, R.J., Aagaard, B.T., Jachens, R.C., and McCabe, C., 2007, Basin structure beneath the Santa Rosa plain, northern California; implications for damage caused by the 1969 Santa Rosa and 1906 San Francisco earthquakes: Bulletin of the Seismological Society of America, v. 97, no. 5, p. 1,449-1,457.

Miller, D.D., 1999, Age of Coast Ranges uplift in Central California, evidence from the sedimentary record of the San Joaquin Basin: American Association of Petroleum Geologists Bulletin, v. 83, no. 4, p. 696-697.

Murphy, L., Fleck, R.J., and Wooden, J.L., 2002, Northbrae Rhyolite in the Berkeley Hills, CA; a rock well-misunderstood: Geological Society of America Abstracts with Programs, v. 34, no. 6, p. 363.

Namson, J., and Davis, T., 1984, Deformational history, thrust-belt structural styles and plate tectonic origin of coast range structures along the San Joaquin Valley, California: Geological Society of America Abstracts with Programs, v. 16, no. 6, p. 607.

Ojakangas, R.W., 1968, Cretaceous sedimentation, Sacramento Valley, California: Geological Society of America Bulletin, v. 79, no. 8, p. 973-1,008.

Page, B.M., 1982, Modes of Quaternary tectonic movement in the San Francisco Bay region, California: California Division of Mines and Geology Special Publication, v. 62, p. 1-10.

Pampeyan, E.H., 1993, Geologic map of the Palo Alto 7-1/2' quadrangle, San Mateo and Santa Clara Counties, California: U.S. Geological Survey Miscellaneous Investigations Series Map I-2371, scale 1:24,000.

Ponce, D.A., Hildenbrand, T.G., and Jachens, R.C., 2003, Gravity and magnetic expression of the San Leandro gabbro with implications for the geometry and evolution of the Hayward Fault zone, northern California: Bulletin of the Seismological Society of America, v. 93, no. 1, p. 1-13.

Ponce, D.A., Simpson, R.W., Graymer, R.W, and Jachens, R.C., 2004, Gravity, magnetic, and seismicity profiles suggest a connection between the Hayward and Calaveras Faults, northern California: Geochemistry, Geophysics, Geosystems - G (super 3), v. 5, no. 7, 39 p.

Roberts, C.W., and Jachens, R.C., 1993, Isostatic residual gravity map of the San Francisco Bay area, California: U.S. Geological Survey Geophysical Investigations Map 1006, scale 1:286,500.

Sarna-Wojcicki, A.M., 1992, Long-term displacement rates on the San Andreas fault system in northern California from the 6-Ma Roblar tuff, *in* Borchardt, Glenn, and others, eds., Earthquake hazards in the eastern San Francisco Bay Area, Proceedings of the 2nd Conference on Earthquake Hazards in the eastern San Francisco Bay Area: California Division of Mines and Geology Special Publication 113, p. 29-30.

Simpson, R.W., Graymer, R.W., Jachens, R.C., Ponce, D.A., and Wentworth, C.M., 2003, Cross-sections and maps showing double-difference relocated earthquakes from 1984-2000 along the Hayward and Calaveras Faults, California: U.S. Geological Survey Open-File Report 2004-1083, version 1.0, [http://pubs.usgs.gov/of/2004/1083/]

Smith, N., 1992, Gravity interpretation of San Pablo Bay and vicinity, *in* Wright, T.L., ed., Field trip guide to Late Cenozoic geology in the north bay region: Northern California Geological Society, p. 71-80.

Suppe, J., 1977, The Coast Range decollement and post-subduction compression in northern California Coast Ranges: Geological Society of America Abstracts with Programs, v. 9, no. 4, p. 510-511.

Unruh, J.R., and Moores, E.M., 1992, Quaternary blind thrusting in the southwestern Sacramento Valley, California: Tectonics, v. 11, no. 2, p. 192-203.

U.S. Census Bureau, 2006, Metropolitan and micropolitan statistical area estimates, [http://www.census.gov/population/www/ehttpstimates/CBSA-est2006-annual.html].

U.S. Geological Survey, 1999, Digitized aeromagnetic datasets for the conterminous United States, Hawaii, and Puerto Rico: U.S. Geological Survey Open-File Report 99-0557, [http://pubs.usgs.gov/of/1999/ofr-99-0557/]

U.S. Geological Survey, 2007, October 21, 1868 Hayward Fault Earthquake [http://earthquake.usgs.gov/regional/nca/1868/].

Vanderhurst, W.L., Cummings, J.C., and Andersen, D.W., 1979, The Santa Clara Formation as evidence of Quaternary uplift and thrusting of the Santa Cruz Mountains, Santa Clara County, California: Geological Society of America Abstracts with Programs, v. 11, no. 3, p. 132.

Waldhauser, Felix, and Ellsworth, W.L., 2000, A double-difference earthquake location algorithm; method and application to the northern Hayward Fault: Bulletin of the Seismological Society of America, v. 90, p. 1,353-1,368.

Waldhauser, Felix, and Ellsworth, W.L., 2002, Fault structure and mechanics of the Hayward Fault, California, from double-difference earthquake locations: Journal of Geophysical Research, v. 107, no. B3, p. 1-15.

Wallace, R.E., 1990, The San Andreas Fault system, California: U.S. Geological Survey Professional Paper 1515, 283 p. [http://pubs.usgs.gov/pp/1990/1515/].

Wentworth, C.M., 1997, General distribution of geologic materials in the San Francisco Bay region, California; a digital map database: U.S. Geological Survey Open-File Report 97-744, 26 p. [http://pubs.usgs.gov/of/1997/of97-744/].

Wentworth, C.M., Blake, M.C. Jr., Jones, D.L., Walter, A.W., Zoback, Mark. D., 1984, Tectonic wedging associated with emplacement of the Franciscan assemblage, California Coast Ranges: Pacific Section Field Trip Guidebook, Society of Economic Paleontologists and Mineralogists, v. 43, p. 163-173.

Williams, R.A., Simpson, R.W., Jachens, R.C., Stephenson, W.J., Odum, J.K., and Ponce, D.A., 2005, Seismic-reflection evidence for a northeast-dipping Hayward Fault near Fremont, California: implications for seismic hazard: Geophysical Research Letters, v. 32, 4 p.

Working Group on California Earthquake Probabilities, 2003, Earthquake probabilities in the San Francisco Bay region; 2003 to 2032: U.S. Geological Survey Open-File Report 03-214, 235 p. [http://pubs.usgs.gov/of/2003/of03-214/].

Wright, T.L., and Smith, N., 1992, Right step from the Hayward Fault to the Rodgers Creek fault beneath San Pablo Bay, *in* Borchardt, G., and others, eds., Proceedings of the Second Conference on earthquake hazards in the eastern San Francisco Bay area: California Department of Conservation, Division of Mines and Geology Special Publication 113, p. 401-417.

Youngman, M.R., 1989, K-Ar and ^{40}Ar/^{39}Ar geochronology, geochemistry, and structural reinterpretation of the southern Sonoma Volcanic field, Sonoma County, California: Berkeley, University of California, M.S. thesis, 92 p., 1 plate.

Appendix I. Data Files

Hayward_Fault_3D_geologic_map: The map is contained in the file "Hayward_3d.enc.faces". The viewer is the executable file "demoviewer.exe." Double-click on the demoviewer.exe file to open the EarthVision™ 3D viewer software and choose the file "Hayward_3d.enc.faces" from the list. For an introduction to using the EarthVision™ 3D viewer tools for the map, see Appendix II. The file is encrypted so that data outside the map volume cannot be viewed.

Virtual Toolkit files:
Virtual Toolkit polygon (.vtp) files are an open-source format that can be viewed in the open-source software Paraview, an alternative to the EarthVision™ 3D viewer. While the entire map is not reconstructed in the .vtp format, each surface in the map (faults and bounding surfaces for geologic units) is available and can be loaded into the Paraview software to be viewed as surfaces. Paraview is available from www.paraview.org. This map was viewed in Paraview 2.4.

The Virtual Toolkit polygon (.vtp) files have the following naming convention:
{*Volume_name*}_{*surface_type*}_{*Surface*}_*#*.vtp
Volume_name is the Fault block name assigned to each unique unit in the 3D map, and can be shown by interactively querying the 3D map (see Appendix II for instructions to query the 3D map).
Surface_type is the type of surface that the file represents, either a fault surface (FS), or a contact or unconformity (ZS).
Surface is the name of the surface, either the name of a fault or the name of a geologic unit within the map.
is a number used for surfaces that have multiple facets associated with the same unit.

Appendix II. Introduction to the Basic EarthVision™ 3D Viewer Tools

How to set viewing parameters and how to query the 3D geologic map of the Hayward Fault

The EarthVision™ 3D viewer is available for Windows XP or Linux. Note that small imperfections may be present in certain views; for example the lines that separate geologic units may disappear, or small artifacts may occur at very high resolution. These artifacts represent the limitations of software and data.

1. To open the EarthVision™ 3D viewer, double-click on the "demoviewer.exe" icon. Single-click on "Hayward_3d.enc.faces" from the list that appears. A "1)" will appear to the left of the name; click on "No more files" at the bottom of the list. If "Hayward_3d.enc.faces" does not appear in the list, navigate to the directory that contains the file, or make sure the file is in the same directory as the file "demoviewer.exe".

2. To access the viewer **main** menu

   The viewer **main** menu is on the right. Sub-menus (such as **manipulate, view**, **zone**) are accessible from the **main** menu. Return to the **main** menu from sub-menus by clicking on the **main** button located at the bottom of the sub-menus.

3. To rotate, pan, and zoom:

   - Rotate the map by using shift-left-click-drag or ctrl-left-click-drag, or the arrow hotkeys, or the azimuth and inclination tools in the **view** menu

   - Pan by using shift-right-click-drag, ctrl-right-click-drag, ctrl-arrow hotkeys, or by using the tools in the **view** menu

   - Zoom in or out by using shift-middle-click-drag, ctrl-middle-click-drag, the "i" and "o" hotkeys, or the tools in the **view** menu

4. To slice the map:

   - From the **manipulate** menu, use the slider bars to slice the map in the X, Y, and Z directions. To slice the model at a given location, left-click on the wire-frame surrounding the model (not displayed in any of the default views – to toggle the wire-frame on and off, use the ctrl-a hotkey or, from the **axes** menu, click the *axes* button (at the top)

5. To add or remove geologic units and fault blocks:

Geologic units
- From the **zone** menu, click on the ***zones-display*** button. A list of all of the geologic units (called ***zones*** in the EarthVision™ software) in the model will appear. Only the units with an asterisk will display.

- Click on one or more geologic units to toggle their display, then click on ***no more zones*** at the bottom of the list. The options ***immediate update, display all zones,*** and ***remove all zones*** are also available.

Fault blocks
- From the **zone** menu, click on the ***fault blocks display*** button. A list of each of the fault-bounded blocks in the model will appear. Only the fault blocks with an asterisk will display.

- Click on one or more fault blocks to toggle their display, then click on ***no more fault blocks*** at the bottom of the list. The options ***immediate update, display all fault blocks,*** and ***remove all fault blocks*** are also available.

6. To change the map colors:

- From the **color** menu, click on the ***color editor button*** and select **zone**. A full-screen color menu will appear; at top the hue, saturation, and level bars are used to choose new colors, the left-hand column shows the current active color set (colors in use in the map are labeled to the right of the column), and in the center is an isolated box that shows the current color.

- First, select the current color. Either left-click on the color bars at top to fill the center box with color, or middle-click on a box in the vertical column and left-click on the center box to fill the center box with a color from the vertical column. Note that the values of the current color are displayed in the top color-bars.

- Second, assign the current color by left-clicking on an appropriate box in the vertical column. Changes can be undone by a second left-button click.

7. To query map features: faults, geologic units, and coordinates:

- From the **3D cursor** menu, click on the ***3D cursor*** button, or use the "k" hotkey. A cursor with three axes that spans the map will appear.

- From the **3D cursor** menu, click on the ***surface snap and query*** button, or use the ctrl-j hotkey, to toggle on the surface query mode.

- Middle-click on some part of the map to snap the cursor to that point and to display information, such as the (x,y,z) coordinate of the cursor, the name of the geologic unit, and the name of the fault block, and the name of the surface.

8. To generate a screen-capture of a view of the map:

- From the **output** menu, left-click on the box that contains the output file format (the default is jpeg). Choose the type of output file from the list.

- Click on the ***specify image size*** button to determine the output file resolution. If the file type is jpeg, enter the compression level from the JPEG Quality box (just under the file format box).

- Click on the ***output file*** button or the ***printer*** button to choose the output option.

- Click on the ***send output*** button and enter filename in the upper window of the menu. A carriage return <CR> saves the file.

9. To display views from map sheet:

- From the **view** menu, click on the ***read view*** button, then select the view file desired from the scroll list (or hit the "e" hotkey to bring up the scroll list). Use the map key "Index of views" in the lower left corner of sheet 1 as a guide.

10. Viewing options can be combined; many other viewing and querying options are available within the viewer. Just explore!